J|A|C|S COMMUNICATIONS

Published on Web 04/10/2009

# High-Field Dynamic Nuclear Polarization in Aqueous Solutions

M. J. Prandolini, V. P. Denysenkov, M. Gafurov, B. Endeward, and T. F. Prisner*

*Institute of Physical and Theoretical Chemistry and Center for Biomolecular Magnetic Resonance, Goethe-University Frankfurt, 60438 Frankfurt am Main, Germany*

Received December 10, 2008; E-mail: Prisner@Chemie.Uni-Frankfurt.de

Sensitivity is a major limitation for structural studies of biomolecules by high-resolution NMR spectroscopy. Recently it was shown that dynamic nuclear polarization (DNP) can be used also at high magnetic fields to strongly enhance solid-state NMR signal intensity.[1] In these experiments polarization of unpaired electron spins was transferred to nuclear spins by solid-state mechanisms (thermal mixing or cross effect),[2,3] which couple electron spins to the nuclear spin reservoir. The situation is more demanding for high-resolution NMR structural studies on biomolecules in solution. First, microwaves mandatory to excite unpaired electrons are strongly absorbed by liquid water samples, and second, the Overhauser polarization transfer mechanism[4] effective for liquids was predicted to be ineffective at high magnetic fields.[5,6] The predicted vanishing spectral densities for dipolar coupling between electron and nuclear spins at high magnetic fields were based on extrapolations of DNP and NMR relaxation measurements performed at magnetic field strengths below 1.5 T.[5−8] As a result only few DNP experiments exist in liquid solutions at high magnetic fields.[9]

Alternatively, DNP has been achieved in the solid phase, and immediately thereafter the sample was liquefied either by rapid dissolution[10] or by laser melting.[11] In liquid samples DNP was performed at a low magnetic field followed by a shuttle of the sample to a high magnetic field for detection.[12] Both of these *ex situ* methods are restricted with respect to repetition of the experiment, because of the physical state changes of the sample within each cycle.

We show here for the first time that unexpected high DNP enhancements of more than 10 can be achieved in liquid water samples at room temperature (RT) and at magnetic fields of 9.2 T (corresponding to 400 MHz $^1$H NMR frequency and 260 GHz EPR frequency). This opens up new possibilities for structural NMR studies on biomolecules with small sample volumes and at physiologically low concentrations.

Our approach is to polarize liquid samples *in situ* at high magnetic fields using a double-resonance structure, which allows simultaneous excitation of the NMR and EPR transitions. The microwave (MW) resonance structure (a $TE_{011}$ cylindrical cavity[13]) was built from a flat helical copper band, which also serves as an NMR coil (for more details see ref 14). The quality factor $Q$ of the MW resonator was 330, loaded with a water filled quartz capillary (0.05 mm inner diameter) and a total sample volume of 3−4 nL. The dimensions of the coupling iris were optimized for water filled capillaries with this diameter. The MW cavity has two important features: first, it drastically reduces the microwave electrical field strength at the sample position, thus avoiding excessive heating of the liquid sample; second, it strongly enhances the MW magnetic field strength at the sample position, which allows significant DNP enhancements already with a very low incident MW power of only 45 mW. The stability of the MW source (purchased from Virginia Diodes Inc.) was improved so that the frequency drift was below $0.5 \times 10^{-5}$ on time scales of our experiment. This improvement has made it possible to measure radicals like Fremy's Salt, which have narrow EPR line widths of less than 0.1 mT at 260 GHz (Figure 1). Additionally, the enhanced frequency stabilization allowed us to improve and quantify the previously measured results on a TEMPOL/water solution.[15] The MW source is connected to the double resonator by a microwave bridge with oversized metal-dielectric waveguides with transmission losses of less than 2 dB (purchased from the Institute of Radiophysics and Electronics, Kharkiv, Ukraine). EPR signals were detected in reflection mode with a zero biased Schottky diode (Virginia Diodes Inc.). The complete MW system was integrated into a standard Bruker 400 MHz NMR spectrometer equipped with a wide-bore magnet.

Figure 1 shows EPR spectra (top) for $^{15}$N Fremy's Salt (left) and $^{15}$N TEMPOL (right) radicals in aqueous solutions at 260 GHz. To improve Fremy's Salt's stability a 0.05 M $K_2CO_3$ buffer was used. The EPR line widths were <0.1 mT and 0.4 mT for Fremy's Salt and TEMPOL, respectively, in aqueous solutions at RT. Corresponding fits to the EPR spectra using EasySpin[16] found a radical rotational correlation time of less than 5 ps (Fremy's Salt) and 20 ps (TEMPOL). Both EPR spectra are well within the motional narrowing limits, for their given $g$-factor anisotropies. The dependence of the EPR amplitude on the square root of the MW power was linear for both Fremy's Salt and TEMPOL, indicating that electron saturation had not been reached at our maximum MW power.

During the DNP experiments, the low field EPR $^{15}$N hyperfine transition was pumped continuously by MW while the NMR free

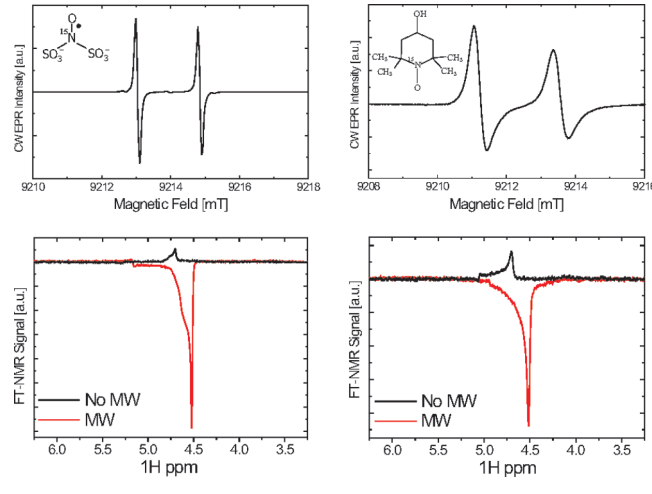


***Figure 1.*** Top: EPR spectrum of 0.6 mM $^{15}$N Fremy's Salt (left) in 0.05 M $K_2CO_3$ and 0.6 mM $^{15}$N TEMPOL (right) in $H_2O$, MW frequency 260 GHz, RT. The structures of the radicals are given as an insert. Bottom: Water proton NMR spectra with MW (red) and without MW (black) pumping at 40 mM and 50 mM radical concentrations for Fremy's Salt (left), TEMPOL (right), respectively.



**10.1021/ja901496g CCC: $40.75** 

induction decay (FID) of the water protons was recorded. The pulsed NMR repetition time was 4 s, and 16 FIDs were averaged for the signal in Figure 1 (bottom, red). The NMR reference spectrum without MW pumping is shown in Figure 1 (bottom, black) for comparison. The experimental DNP enhancement is calculated by $\epsilon = (\nu_{MW} - \nu_0)/\nu_0$, where $\nu_{MW,0}$ are integrated NMR signal intensities with and without MW, respectively. The corresponding enhancements are −10.4(10) for Fremy's Salt and −6.2(6) for TEMPOL. The negative enhancement confirms that the Overhauser effect is mediated predominantly via electron−proton dipole−dipole relaxation.[5,6]

The frequency shift of the water proton NMR peak is caused by MW heating (Figure 1, bottom). Under continuous MW irradiation, the temperature becomes stable at a higher value in less than a second. The amount of heating is related to the size of the capillary; for the sizes 0.05/0.03 mm i.d. the temperature increases approximately 20/10 K, at our maximum MW power, respectively. The experiment was performed without any active cooling, which will be implemented in a new probe. The broad NMR line shape of 130 Hz is caused by static magnetic field inhomogeneity across the sample (discussed in ref 15). Although this value does not yet allow high-resolution NMR applications, the field inhomogeneity in our present design does not affect our obtained DNP enhancement results.

The DNP build-up time was measured to be on the order of the water proton $T_1$ with radicals, as predicted by the Solomon equations.[5,6,15] The water-proton relaxation rate dependence on the radical concentration is given by $R_1 = 1/T_{1W} + kC$, where $k$ is the relaxivity, $C$ is the concentration in mM, and $T_{1W}$ is the relaxation of pure water. The relaxivity constants were found to be 0.068(8), and 0.09(1) $s^{-1}$ $mM^{-1}$, for Fremy's Salt and TEMPOL, respectively, and $T_{1W}$ is 4.8(4) s at 318 K (this is the temperature at maximum MW power). While at room temperature, TEMPOL has a relaxivity of 0.16(2) $s^{-1}$ $mM^{-1}$ and the $T_{1W}$ of pure water is 3.3(2) s. The dependence of the DNP enhancement at maximum MW power for both radicals is depicted in Figure 2.

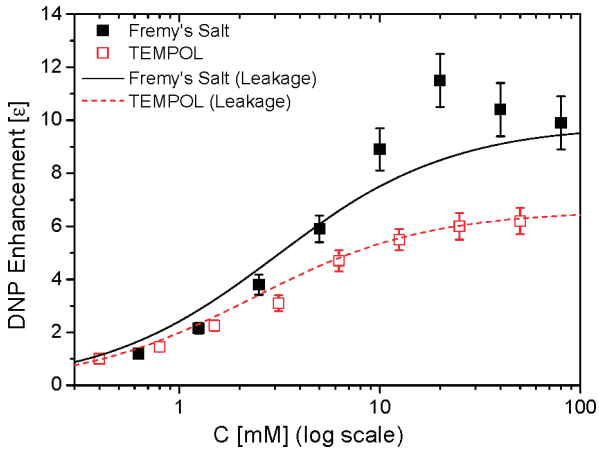


***Figure 2.*** Dependence of the DNP enhancement at maximum MW power on the radical concentration (Fremy's Salt (black) and TEMPOL (red)). As a comparison, the dependence of the leakage factor $f$ on concentration has been scaled to the DNP enhancement data points.

Figure 3 shows the power curves for Fremy's Salt and TEMPOL in aqueous solutions, which is the dependence of the inverse enhancement $\epsilon$ on the inverse MW power. The small deviation from a linear relation at high MW power might be caused by the MW heating described above, which shortens the translational radical/water correlation time and, thereby, increases the DNP effect. Fitting only the lower power values where the sample is near room temperature, a maximum extrapolated DNP enhancement $\epsilon_{MAX}$ at saturating power can be estimated: −7.7(±1.0) for Fremy's Salt and −14(+8/−2) for TEMPOL.

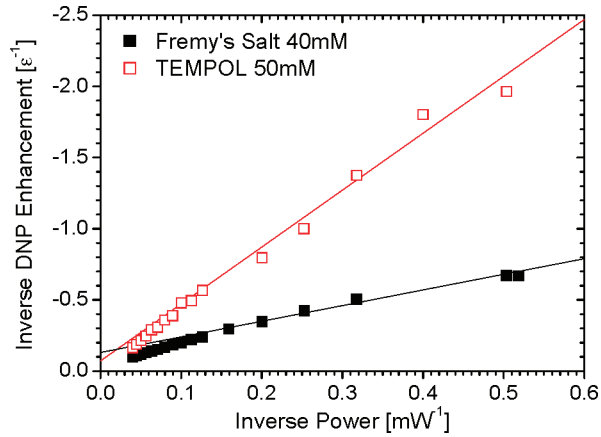


***Figure 3.*** Dependence of the inverse enhancement ($\epsilon$) on the inverse power for the radicals Fremy's Salt and TEMPOL. The maximum extrapolated DNP enhancements are given by a linear fit to the data at lower MW powers.

The Overhauser enhancement, $\epsilon$, is usually factorized into

$$\varepsilon = (\gamma_e/\gamma_p)\xi s f \qquad (1)$$

where $\gamma_e$ and $\gamma_p$ are the gyromagnetic ratios of the electron and proton, respectively, $\xi$ is the DNP coupling constant, $f = 1 - 1/(R_1 T_{1W})$ is the leakage factor, and $s$ is the degree of electron saturation. The leakage factor $f$ was easily determined experimentally, by measuring the water-proton relaxation time with $(1/R_1)$ and without radicals ($T_{1W}$). The other two parameters, $s$ and $\xi$, are more difficult to obtain.

The strong dependence of the DNP enhancement on the radical concentration can be mainly explained by the leakage factor, $f$, as shown in Figure 2. Deviation from this behavior has been attributed to Heisenberg exchange, which influences the electronic relaxation times and thereby the ability to saturate the electron spin. The leakage factor has been also plotted in Figure 2 and is scaled (Fremy's Salt 0.7$f$ and TEMPOL 0.47$f$) to the DNP enhancement data points. While TEMPOL shows a monotonically increasing behavior, Fremy's Salt shows a maximal DNP enhancement of −11.5(10) at 20 mM and decreases at higher concentrations. Modeling the dependence of the measured DNP enhancement on concentration has proved to be a nontrivial problem.[5−7] In comparison to our results, the observed DNP enhancement of TEMPOL at lower microwave frequencies (X-band: 9.8 GHz) shows a maximum enhancement between 6 to 8 mM.[7]

The saturation expression for a homogeneously broadened single EPR line is given by $s = \gamma_e^2 B_2^2 T_{1e} T_{2e}/(1 + \gamma_e^2 B_2^2 T_{1e} T_{2e})$, where $B_2$ is the strength of the MW field and $T_{1e,2e}$ are the electronic spin−lattice and spin−spin relaxation times. In this expression, the product $T_{1e}T_{2e} = 35 \times 10^{-16}$ $s^2$ had been estimated from an EPR power saturation curve for a TEMPOL/water solution at 260 GHz.[14] Together with $T_{2e} = 28$ ns, calculated from the EPR line width (see Figure 1), $T_{1e}$ is estimated to be approximately 120 ns at 260 GHz and RT. Direct determination of electronic relaxation times by EPR have not yet been performed for such high frequencies, but our results are in good agreement with EPR results obtained at 95 GHz.[17,18] A similar $T_{1e}$ is predicted for Fremy's Salt by comparison of the two slopes in Figure 3 and by taking the different EPR line widths into account.

Although the Fremy's Salt solution gave higher enhancements at all MW power levels, Figure 3 predicts similar projected maximum enhancements $\epsilon_{MAX}$ for both radicals at MW saturation. Therefore, the difference in the observed enhancements for Fremy's Salt and TEMPOL can be mainly attributed to a difference in the saturation factor $s$, whereas the coupling factor $\xi$ seems to be similar for both radicals.

In the past, DNP enhancement and NMR relaxation dispersion measurements performed at lower magnetic field values have been used to predict the spectral density function of the dipole−dipole interaction. The analysis was usually based on a model assuming free diffusion and a spherical radical (force-free model).[19] From X-band (9.8 GHz) DNP measurements with TEMPONE in water a coupling factor $\xi = 0.186$ was determined,[7] leading to a correlation time of 95 ps. These results were in good agreement with NMR relaxation dispersion measurements,[8] which estimated a correlation time of 73 ps with TEMPAMINE in water. If we predict the coupling factor at 260 GHz from this value and the model described above, we end up with a maximum enhancement at 260 GHz of only 1.6 (assuming $s = f = 1$). This is obviously much lower than the experimentally extrapolated maximum enhancement of 14. More recent relaxation dispersion measurements on TEMPOL in water[20,21] predicted coupling factors $\xi$ of 0.36 (X-band) and 0.06 (W-band), corresponding to much shorter correlation times of 25 ps (X-band) and 28 ps (W-band). Using their parameters and our measured relaxivity at 260 GHz, we can estimate a coupling factor of $\xi = 0.022(6)$ and a correlation time of 20 ps at 260 GHz. This would correspond to a maximum enhancement of approximately 14, in excellent agreement with our experimentally obtained values.

Our experimental DNP enhancements on TEMPOL in water at 260 GHz show much higher coupling factors than predicted by DNP experiments performed at lower magnetic field strengths. The discrepancy might be either due to difficulties in determining the saturation factor $s$ for nitroxide radicals accurately or a result of a more complex behavior of the spectral density function than predicted from the force-free model. In particular our high-field DNP experiments will be very sensitive to dynamical processes in the low picoseconds time scale. More elaborate investigations to quantify the coupling factor and the radical electron/water proton correlation times using molecular dynamic simulations are underway.

Additionally, our results demonstrate that Fremy's Salt gives significant DNP enhancements of −10 at very low MW power levels, because of its long electronic relaxation time $T_{2e}$. Even larger enhancements will be achievable on both radicals with higher MW power and at slightly higher temperatures. Pulsed MW at a spacing similar to $T_{1e}$ of the radical might even double the achieved enhancement on water.[22] With an initial starting water polarization of 10 or more, the chances to further transfer a substantial amount of this polarization onto biomolecules are high. This transfer from polarized solvent protons to the biomolecule might be accomplished by direct proton exchange with liable NH or OH groups, through NOE polarization transfer between solvent and biomolecule protons or by directly attaching the spin label to the protein. Developments to improve the field homogeneity at the sample and to increase the effective sample size are underway which will allow application of the method to biomolecules. Our results therefore demonstrate the first important step toward the application of DNP to structural investigations of biomolecules in the liquid state.

**Acknowledgment.** The work has been financially supported by the European Design Study BIO-DNP and the Center of Biomolecular Magnetic Resonance, Frankfurt. We thank F. Engelke and A. Krahn for support with the NMR probe, J. Törring for the construction of the field sweep program, D. Margraf for synthesizing Fremy's Salt, B. Thiem for improvement of mw-source stability, and S. Lyubenova and D. Sezer for his scientific advice.

**References**

(1) Maly, T.; Debelouchina, G. T.; Bajaj, V. S.; Hu, K.-N.; Joo, C.-G.; Mak-Jurkauskas, M. L.; Sirigiri, J. R.; van der Wel, P. C. A.; Herzfeld, J.; Temkin, R. J.; Griffin, R. G. *J. Chem. Phys.* **2008**, *128*, 052211.
(2) Abragam, A.; Goldman, M. *Rep. Prog. Phys.* **1978**, *41*, 395–467.
(3) Atsarkin, V. A. *Sov. Phys. Usp.* **1978**, *21*, 725–745.
(4) Overhauser, A. W. *Phys. Rev.* **1953**, *92*, 411–415.
(5) Hausser, K. H.; Stehlik, D. *Adv. Magn. Reson.* **1968**, *3*, 79–139.
(6) Müller-Warmuth, W.; Meise-Gresch, K. *Adv. Magn. Reson.* **1983**, *11*, 1–45.
(7) Armstrong, B. D.; Han, S. *J. Chem. Phys.* **2007**, *127*, 104508.
(8) Borah, B.; Bryant, R. G. *J. Chem. Phys.* **1981**, *75*, 3297–3300.
(9) Loening, N. M.; Rosay, M.; Weis, V.; Griffin, R. G. *J. Am. Chem. Soc.* **2002**, *124*, 8808–8809.
(10) Ardenkjaer-Larsen, J. H.; Fridlund, B.; Gram, A.; Hansson, G.; Hansson, L.; Lerche, M. H.; Servin, R.; Thaning, M.; Golman, K. *Proc. Natl. Acad. Sci. U.S.A.* **2003**, *100*, 10158–10163.
(11) Joo, C.-G.; Hu, K.-N.; Bryant, J. A.; Griffin, R. G. *J. Am. Chem. Soc.* **2006**, *128*, 9428–9432.
(12) Reese, M.; Lennartz, D.; Marquardsen, T.; Höfer, P.; Tavernier, A.; Carl, P.; Schippmann, T; Bennati, M.; Carlomagno, T.; Engelke, F.; Griesinger, C. *Appl. Magn. Reson.* **2008**, *34*, 301–311.
(13) Weis, V.; Bennati, M.; Rosay, M.; Bryant, J. A.; Griffin, R. G. *J. Magn. Reson.* **1999**, *140*, 293–299.
(14) Denysenkov, V. P.; Prandolini, M. J.; Krahn, A.; Gafurov, M.; Endeward, B.; Prisner, T. F. *Appl. Magn. Reson.* **2008**, *34*, 289–299.
(15) Prandolini, M. J.; Denysenkov, V. P.; Gafurov, M.; Lyubenova, S.; Endeward, B.; Bennati, M.; Prisner, T. F. *Appl. Magn. Reson.* **2008**, *34*, 399–407.
(16) Stoll, S.; Schweiger, A. *J. Magn. Reson.* **2006**, *178*, 42–55.
(17) Froncisz, W.; Camenisch, T. G.; Ratke, J. J.; Anderson, J. R.; Subczynski, W. K.; Strangeway, R. A.; Sidabras, J. W.; Hyde, J. S. *J. Magn. Reson.* **2008**, *193*, 297–304.
(18) Hofbauer, W.; Earle, K. A.; Dunnam, C. R.; Moscicki, J. K.; Freed, J. H. *Rev. Sci. Instrum.* **2004**, *75*, 1194–1208.
(19) Freed, J. H. *J. Chem. Phys.* **1978**, *68*, 4034–4037.
(20) Luchinat, C.; Parigi, G. *Appl. Magn. Reson.* **2008**, *34*, 379–392.
(21) Höfer, P; Parigi, G.; Luchinat, C.; Carl, P.; Guthausen, G.; Reese, M.; Carlomagno, T.; Griesinger, C.; Bennati, M. *J. Am. Chem. Soc.* **2008**, *130*, 3254–3255.
(22) Un, S.; Prisner, T.; Weber, R. T.; Seaman, M. J.; Fishbein, K. W.; McDermott, A. E.; Singel, D. J.; Griffin, R. G. *Chem. Phys. Lett.* **1992**, *189*, 54–59.

JA901496G